Available online at www.sciencedirect.com
SCIENCE DIRECT®
ELSEVIER
International Journal of Multiphase Flow 30 (2004) 291–310
International Journal of Multiphase Flow
www.elsevier.com/locate/ijmulflow

An investigation on void fraction of vapor–liquid two-phase flow for smooth and microfin tubes with R134a at adiabatic condition

Shigeru Koyama [a,*], Joodong Lee [b], Ryuuichirou Yonemoto [b]

[a] *Institute for Materials Chemistry and Engineering, Kyushu University, Kasuga-koen 6-1, Kasuga 816-8580, Japan*
[b] *Department of Energy and Environmental Engineering, Interdisciplinary Graduate School of Engineering Sciences, Kyushu University, Kasuga-koen 6-1, Kasuga 816-8580, Japan*

Received 21 May 2003; received in revised form 8 September 2003

Abstract

The present paper deals with experiments and a prediction method for the void fraction of R134a vapor–liquid two-phase flow in horizontal smooth and microfin tubes in adiabatic condition. The void fraction is measured by the quick closing valve method. The smooth tube tested is 1024 mm in length and 7.52 mm in inside diameter. The microfin tube tested is 1015 mm in length and 8.86 mm in mean inside diameter; the fin height is 0.18 mm, the helix angle of fins is 25° and the total number of fins are 70. The experiments were carried out in the range of vapor quality from 1% to 96%, where the pressure was kept at 1.2 and 0.8 MPa and the mass flow rate was kept at 20 and 40 kg h^{-1}. It is confirmed that the void fraction for smooth tube is well correlated by the Smith or the Baroczy correlations. It is also shown that the void fraction in the microfin tube is lower than that of smooth tube in any quality and the prediction results using previous correlations for smooth tube are higher than the present experimental data of microfin tube. The void fraction prediction method consisting of a stratified-annular flow model and an annular flow model is proposed. In the stratified-annular flow model, it is assumed that most of liquid flows at the bottom of the tube and all grooves are filled with additional liquid. The momentum equations are constructed for regions of vapor, main liquid flow at the bottom and additional liquid flow in grooves, respectively. These coupled equations are solved numerically. In the case of annular flow model, it is assumed that all grooves are filled with liquid uniformly. The momentum equations in the vapor and liquid flows in grooves are also solved numerically. The values of the predicted void fraction are in good agreement with experimental data in high

* Corresponding author. Tel.: +81-92-583-7831; fax: +81-92-583-7833.
E-mail address: koyama@cm.kyushu-u.ac.jp (S. Koyama).

0301-9322/$ - see front matter
doi:10.1016/j.ijmultiphaseflow.2003.10.009

vapor quality region, while the predicted values are slightly smaller than experimental ones in low vapor quality region.

Keywords: Void fraction; Microfin tube; Smooth tube; R134a; Adiabatic condition; Slip ratio; Two-phase flow

1. Introduction

The void fraction is one of the important parameters in heat transfer and flow characteristics for vapor–liquid two-phase flow. It is worthwhile to predict the void fraction in a microfin tube as a function of the design and operating parameters of the heat exchanger and calculating the amount of refrigerant charge in evaporator and condenser since most of the air-conditioning systems adopt microfin tubes to improve their efficiency over the past two decades. However, there are few studies found in the literature and the characteristics of void fraction in a microfin tube are not clarified yet. Moreover, most investigations on void fraction are limited for air water two-phase flow on smooth tube. Therefore, the investigations on void fraction for microfin tubes become more attractive and important. Up to now, only limited studies on void fraction for microfin tube can be found in open literatures. Yashar et al. (2001) carried out experiments on the void fraction of R134a and R410A condensing and evaporating in smooth and microfin tubes and proposed an empirical correlation for microfin tube.

Over the years, some representative examples of correlations and models of void fraction in a smooth tube are as follows: Lockhart and Martinelli (1949) first attempted to predict the void fraction in a smooth tube. Butterworth (1975) reviewed a number of studies on void fraction for co-current gas–liquid flow in smooth tube. Rice (1987) also gave a brief overview of previous correlations of void fraction in smooth tube. He classified four categories: the homogeneous model, the slip ratio based model, the Lockhart–Martinelli parameter correlated model and the mass flux dependent model.

The Homogeneous model is the simplest one for calculating void fraction in two-phase flow, in which the vapor and liquid phases are treated as a homogeneous mixture flowing with same velocity. This model is usually recognized as an ideal case and upper limit to the complex two-phase flow.

Levy (1960), Zivi (1964), Thom (1964) and Smith (1971) proposed the slip ratio based models. The slip ratio based model is that the flow is segregated into vapor and liquid streams. Levy analyzed the problems of steam slip in forced circulation of boiling water and developed a simplified momentum model to obtain a theoretical prediction of steam slip and two-phase pressure drop. Zivi made an analysis of void fraction of steady-state steam by means of the principle of minimum entropy production. He assumed that energy dissipation due to wall friction in the channel was negligible and the flow pattern was fully annular with no liquid entrained in the vapor. He discussed the effect of wall shear stress and entrainments to void fraction and pressure drops, respectively. He pointed out that wall friction reduced the void fraction and increased the slip ratio. Thom obtained an empirical relationship between quality and void fraction based on the assumption that the slip ratio is constant at a given pressure. Smith also developed a slip ratio based correlation of void fraction employing an equal velocity head model. He stated that his

correlation was valid for all conditions of two-phase flow irrespective of the pressure, mass velocity, flow regime and rate of change of enthalpy.

Baroczy (1966) and Wallis (1969) proposed the prediction correlations of void fraction utilizing the Lockhart and Martinelli parameter. Baroczy carried out experiments for isothermal, two-phase of liquid mercury–nitrogen and water–air and presented void fraction data as a function of the Lockhart and Martinelli parameter. Wallis obtained the correlation of void fraction at low pressures using the data of Lockhart and Martinelli. He pointed out that his method led to progressively increasing errors as the frictional component of pressure drop decreases in proportion to the other terms.

Hughmark (1962) and Premoli et al. (1971) obtained empirically based correlations including the mass flux effect and Tandon et al. (1985) developed the mass flux dependent model of void fraction for annular flow analytically.

As mentioned above, the detailed information on void fraction for two-phase flow in microfin tubes are unavailable. In this paper, experiments on void fraction of R134a vapor–liquid two-phase flow are conducted for both smooth and microfin tubes at adiabatic condition. A comparison of void fraction between smooth and microfin tubes is performed. The experimental data for both smooth and microfin tubes are compared with previous correlations, most of which are proposed for smooth tubes. A method to predict the void fraction for microfin tube with R134a at adiabatic condition is also proposed.

2. Experimental facilities

2.1. Experimental apparatus and procedure

Fig. 1 shows the schematic view of the experimental apparatus, which consists of three loops: a refrigerant loop, a water loop and a brine loop. In the refrigerant loop, subcooled refrigerant liquid is delivered with a magnetic gear pump (1) through a desiccant filter (2), a mass flow meter (3), a pre-heater (4) and a mixing chamber (5) to a heat exchanger (6). The pre-heater (4) and the heat exchanger (6) are used to heat the refrigerant liquid close to the saturation state. Then, the refrigerant flows through an evaporator (10) into the test section for the measurement of the void fraction (11). The evaporator (10), around which an electrical heater is wrapped, is used to regulate the vapor quality at the entrance of the test section (11). The refrigerant flowing from the test section returns through a visualization section for observation of the flow pattern (12), an after-heater (14) and two condensers (15, 16) to the pump (1). The after-heater (14) and two condensers (15, 16) are used to adjust the refrigerant pressure level in the refrigerant loop. The water loop, which consists of a heat source tank (7), a centrifugal pump (8) and a gear-type flow meter (9), is used to supply heating water to the heat exchanger (6). The brine loop, that consists of a brine tank (18), three centrifugal pumps (8), two float-type flow meters (19) and a chilling unit (20), is used to condense the refrigerant.

The refrigerant mass flow rate is measured using the mass flow meter with ±0.5% resolution of measured value. Pressures at inlet and outlet of the evaporator and the test section are measured using an absolute pressure transducer with a resolution of ±0.1% of a full scale. Refrigerant

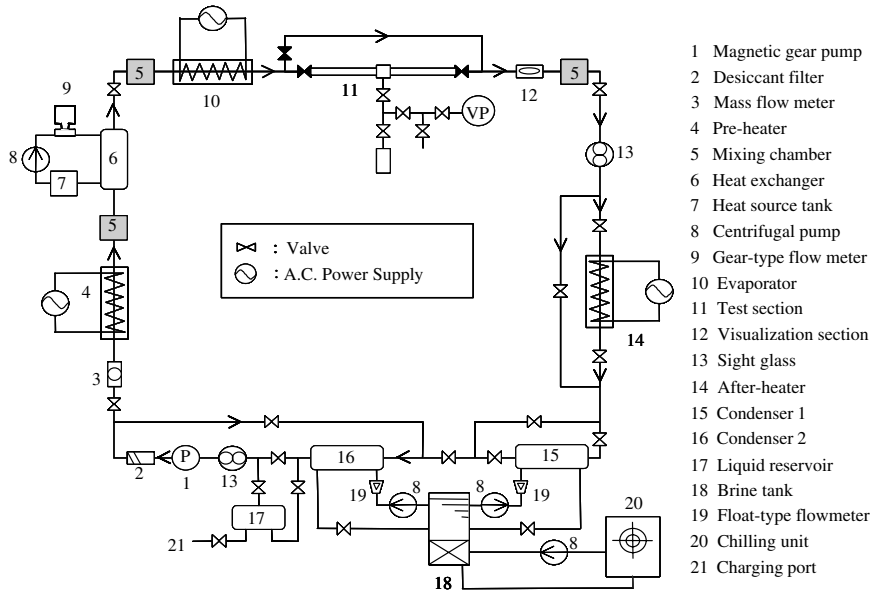

Fig. 1. Schematic diagram of the experimental apparatus.

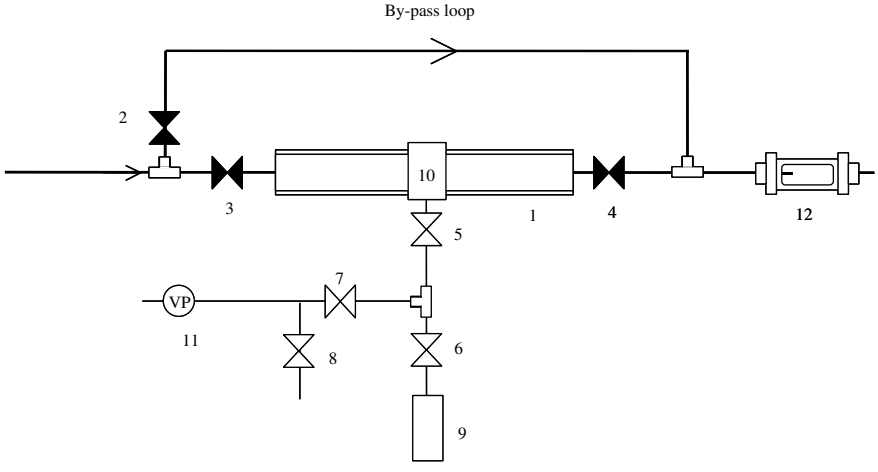

Fig. 2. Schematic diagram of the test section.

temperatures in the refrigerant loop are measured using several 0.5 mm sheathed K-type thermocouples, which were calibrated in advance within an error of ±0.05 K.

Fig. 2 shows the schematic view of the test section for the measurement of the void fraction. The test section consists mainly of a test tube (1), a bypass loop, three valves with air actuators (2,

3, 4), a sampling vessel (9), a sampling port (10) and a vacuum pump (11). The void fraction of two-phase flow is measured by means of simultaneously closing valves. It is noted that the void fraction is measured on the adiabatic condition. The operating procedures of this measurement are as follows:

(1) Valves (2), (5), (7) and (8) are closed, while the others are opened. The temperature of the sampling vessel (9) is kept around 273 K using an icebox to collect refrigerant of test tube easily with condensing process.
(2) After opening the valve (7), the sampling vessel (9) including the piping is evacuated with the vacuum pump (11). Then, the valve (7) is closed again.
(3) The refrigerant temperature and pressure in the test tube (1) are measured at the sampling port (10). The refrigerant flow rate, the heat transfer rate in the evaporator, and the refrigerant pressure and temperature in the refrigerant loop are also measured.
(4) Valves (3) and (4) are closed with air actuators instantaneously. Difference in closing time between valves (3) and (4) is estimated to be within 0.1 s. At the same time, the valve (2) is opened.
(5) Valve (5) is opened. Then, the refrigerant is condensed and collected in the sampling vessel (9). After that, valve (6) is closed.
(6) The refrigerant temperature and pressure in the test tube are measured again at the sampling port (10) to evaluate the amount of the remaining refrigerant vapor in the test tube.
(7) The weight of the sampling vessel (9) containing the refrigerant is measured with an accurate electrical balance of ±1 mg resolution. Then, the net weight of refrigerant is obtained.

2.2. Data reduction method

The void fraction, ε, is obtained from the following equation:

$$\varepsilon = \frac{V_G}{V_G + V_L} = \frac{\rho_L V - m}{(\rho_L - \rho_G)V}, \tag{1}$$

where V_L is the liquid volume of the test tube, V_G is the vapor volume of the test tube and V is the total volume of the test tube. The mass of the refrigerant existing in the test tube before closing valves (3) and (4) in Fig. 2, m, is calculated as

$$m = m' + \rho'_G V', \tag{2}$$

where m' is the refrigerant mass in the sampling vessel (9) in Fig. 2, ρ'_G is the superheated vapor density in the test tube after collection process and V' is the volume of the test tube and the piping between the sampling port and valves (6, 7) in Fig. 2.

The quality of refrigerant at the inlet of the test tube, x, is evaluated from

$$x = \frac{h_b - h_{L,sat}}{h_{G,sat} - h_{L,sat}}, \tag{3}$$

where $h_{L,sat}$ is the liquid specific enthalpy at the saturated state and $h_{G,sat}$ is the vapor specific enthalpy at the saturated state. The bulk refrigerant specific enthalpy at the inlet of the test tube, h_b, is calculated by

$$h_b = \frac{(Q - Q_{loss})}{W} + h_{b0}, \tag{4}$$

where Q is the heat transfer rate in the evaporator, Q_{loss} is the heat loss from the evaporator to the ambience, W is the mass flow rate of refrigerant and h_{b0} is the bulk refrigerant specific enthalpy at the inlet of the evaporator.

The thermal physical properties of R134a are determined from the program package REFPROP Version 6.0 (1998).

2.3. Experimental conditions

In the present study, commercially available smooth and microfin tubes made of copper were used as test tubes. The inside surface of the microfin tube is grooved spirally. The dimensions of the test tubes are summarized in Table 1, where "area enlargement ratio" is defined as the ratio of a real inside surface area to that of smooth tube having the same inside diameter as mean inside diameter of the microfin tube.

Experiments for void fraction have been conducted using refrigerant R134a as the working fluid in the ranges shown in Table 2. All of the data signals have been collected and recorded by a data acquisition system.

The reliability in the measurement of void fraction by a quick closing valve method is affected by three factors, which are the degree of superheat of remaining vapor in the test tube after collection process, the length of the test tube and the volume of the sampling vessel. Prior to the void fraction experiments, these effects were confirmed by preliminary experiments.

(1) If a part of the liquid remains in the test tube and the piping after collection process, the measured temperature is close to the saturation temperature that is calculated from the measured pressure in the test section. To omit data obtained these conditions, in which the degree of superheat of the vapor in the test tube and the piping after collection process is higher than 20 K, are selected.

Table 1
Dimension of smooth and microfin tubes

Item	Unit	Microfin tube	Smooth tube
		Scale	Scale
Outside diameter	mm	9.52	9.52
Mean inside diameter	mm	8.86	7.52
Minimum inside diameter	mm	8.60	7.52
Number of fins	–	70	–
Helix angle	Degree	25	–
Fin height	mm	0.18	–
Fin top angle	Degree	25	–
Mean wall thickness	mm	0.33	–
Minimum wall thickness	mm	0.28	–
Area enlargement ratio	–	1.67	–
Test tube's length	m	1.015	1.024

Table 2
Experimental ranges

	Smooth tube		Microfin tube	
Inlet pressure (MPa)	0.8	1.2	0.8	1.2
Mass velocity ($kg\,m^{-2}\,s^{-1}$)	125, 250	125, 250	90, 180	90, 180
Inlet temperature (K)	301–305	313–317	301–305	313–317

Table 3
Uncertainty analysis of vapor quality and void fraction

	P (MPa)	G ($kg\,m^{-2}\,s^{-1}$)	x	ε	U_x	U_ε
Smooth tube	1.2	250	0.02	0.32	0.009	0.056
			0.94	0.95	0.077	0.008
		125	0.03	0.38	0.017	0.051
			0.92	0.95	0.15	0.008
	0.8	250	0.001	0.21	0.004	0.062
			0.85	0.94	0.067	0.007
		125	0.04	0.49	0.012	0.041
			0.86	0.94	0.134	0.007
Microfin tube	1.2	180	0.007	0.11	0.014	0.053
			0.91	0.91	0.083	0.008
		90	0.07	0.37	0.028	0.038
			0.95	0.90	0.16	0.009
	0.8	180	0.02	0.38	0.009	0.037
			0.84	0.91	0.07	0.007
		90	0.06	0.38	0.015	0.037
			0.93	0.91	0.15	0.007

(2) About 1 m in length of the test tube was selected after preliminary experiments as changing length of the test tube.
(3) The sampling vessel of a volume 150 cm^3 was selected to cover the amount of refrigerant of the test tube sufficiently. If the volume of the sampling vessel is not enough, a part of liquid may remain in the test tube and the piping after the collection process.

An uncertainty analysis has been performed according to the method proposed by Moffat (1988). Table 3 shows the uncertainties of vapor quality and void fraction with typical cases of test data in both smooth and microfin tubes, where U_x and U_ε are the uncertainties of vapor quality and void fraction, respectively. Uncertainties of the vapor quality and void fraction in the present study are estimated to be ±0.16 and ±0.06 in maximum, respectively.

3. Experimental results and discussion for smooth and microfin tubes

Experimental data of void fraction for both smooth and microfin tubes were obtained for the range of vapor quality from 1% to 96%. The present experimental data are compared to the past

studied representative correlations for void fraction in smooth and microfin tubes, which are summarized in Table 4, where E is the ratio of mass of water flowing in homogeneous mixture to total mass of water flowing, F_t is the Froude rate, G is the mass velocity, Re_L is the liquid Reynolds number, X or X_{tt} is the Lockhart–Martinelli parameter, v_G is the specific volume of saturation vapor, v_L is the specific volume of saturation liquid, η_G is the viscosity of saturation vapor and η_L is the viscosity of saturation liquid.

Prior to the experiments for microfin tube, the void fraction of smooth tube was measured at adiabatic conditions to check the reliability of experimental systems. Fig. 3 shows the experimental results of void fraction for smooth tube. In this figure opened and closed symbols denote the results for $P = 1.2$ and 0.8 MPa, respectively. In each symbol the difference of mass velocity is distinguished by circle and triangle symbols. The effect of refrigerant pressure on the void fraction is significant, while that of mass velocity is very small especially for high vapor quality region. This means that the void fraction is mainly affected by the physical properties of refrigerant. All the data of void fraction approach to unity as the vapor quality closes to unity.

Fig. 4(a) and (b) show the comparison between the experimental data and several correlations for void fraction in smooth tube for $P = 1.2$ and 0.8 MPa, respectively. Symbols of circle and triangle represent experimental data for $G = 250$ and 125 $\mathrm{kg\,m^{-2}\,s^{-1}}$, respectively. A dotted line, a dashed line, a chain line, a double dotted chain line, a thick solid line and a thin solid line represent the correlations of the homogeneous model, Smith (1971), Zivi (1964), Baroczy (1966), Tandon et al. (1985), ($G = 250$ $\mathrm{kg\,m^{-2}\,s^{-1}}$) and Tandon et al. (1985) ($G = 125$ $\mathrm{kg\,m^{-2}\,s^{-1}}$), respectively. The homogeneous model indicates the highest value of void fraction, which overpredicts the void fraction compared with the present experimental data. The Smith correlation is in good agreement with the present experimental data for smooth tube. The Zivi correlation shows a lower void fraction at low quality region and higher value at high quality region compared with experimental data. The Baroczy correlation is good agreement with the present experimental results for smooth tube. The Tandon et al. correlation show a little higher value than present experimental data. As a result, the Smith and the Baroczy correlations agree with the present experimental data with ±10% discrepancy.

Fig. 5 shows the experimental results of void fraction for microfin tube. In this figure opened and closed symbols denote the results for $P = 1.2$ and 0.8 MPa, respectively. In each symbol the difference of mass velocity is distinguished by circle and triangle symbols. The void fraction increases with the decrease of the refrigerant pressure. This trend is similar to that of smooth tube. The void fraction increases with the increase of mass velocity. This effect is more remarkable as the refrigerant pressure or the vapor quality decreases. It is noted that in the case of smooth tube this effect is negligible as can be seen from Fig. 3. It is not observed from the present data that the void fraction do not approach to unity as the vapor quality closes to unity for microfin tube. However, it is inferred that the void fraction for microfin tube is supposed to be close to unity sharply as vapor quality approaches adjacent to unity.

As a trial, the experimental data of void fraction in microfin tube are compared with several correlations for smooth tube and the correlation of Yashar et al. for microfin tube. Fig. 6(a) and (b) show the comparison of void fraction between the experimental data in microfin tube and several correlations in smooth for $P = 1.2$ and 0.8 MPa, respectively. Symbols of circle and triangle represent experimental data in cases of $G = 180$ and 90 $\mathrm{kg\,m^{-2}\,s^{-1}}$, respectively. A dotted

Table 4
Summary of previous correlations of the void fraction for smooth and microfin tubes

Authors	Correlations	
Homogeneous model	$\varepsilon = x \cdot \left[x + (1-x)\dfrac{\rho_G}{\rho_L} \right]^{-1}$	–
Zivi (1964)	$\varepsilon = x \cdot \left[x + (1-x) \cdot (\rho_G/\rho_L)^{(2/3)} \right]^{-1}$	
Baroczy (1966)	$\varepsilon = \left[1 + \left(\dfrac{1-x}{x} \right)^{0.74} \cdot \left(\dfrac{\rho_G}{\rho_L} \right)^{0.65} \cdot \left(\dfrac{\eta_L}{\eta_G} \right)^{0.13} \right]^{-1}$ (Burttworth rearranged)	
Smith (1971)	$\varepsilon = \left\{ 1 + \dfrac{\rho_G}{\rho_L} \cdot E \cdot \left(\dfrac{1}{x} - 1 \right) + \dfrac{\rho_G}{\rho_L} \cdot (1-E) \cdot \left(\dfrac{1}{x} - 1 \right) \left[\dfrac{\frac{\rho_L}{\rho_G} + E \cdot \left(\frac{1}{x} - 1 \right)}{1 + E \cdot \left(\frac{1}{x} - 1 \right)} \right]^{1/2} \right\}^{-1}$	Smooth tube
Tandon et al. (1985)	$\varepsilon = 1 - 1.928 Re_L^{-0.315} [F(X_{tt})]^{-1} + 0.9293 Re_L^{-0.63} [F(X_{tt})]^{-2}, \quad 50 < Re_L < 1125$ $\varepsilon = 1 - 0.38 Re_L^{-0.088} [F(X_{tt})]^{-1} + 0.0361 Re_L^{-0.176} [F(X_{tt})]^{-2}, \quad Re_L > 1125$ $F(X_{tt}) = 0.15 [X_{tt}^{-1} + 2.85 X_{tt}^{-0.476}]$	
Yashar et al. (2001)	$\varepsilon = (1 + F_t^{-1} + X_{tt})^{-0.321}$ $F_t = \left(\dfrac{G^2 x^3}{(1-x)\rho_G^2 g d_i} \right)^{0.5}$	Microfin tube

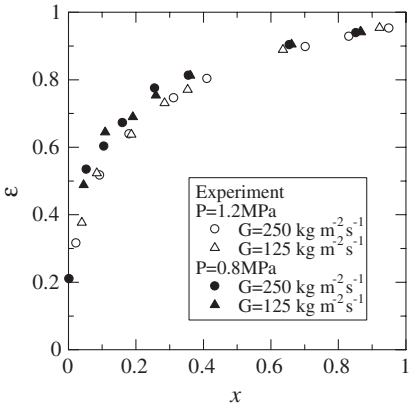

Fig. 3. Experimental results of void fraction for a smooth tube.

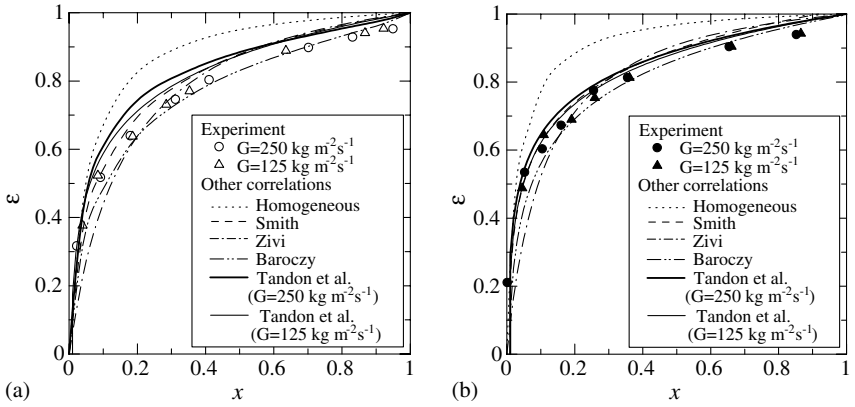

Fig. 4. Comparison between present experimental results and previous correlations for a smooth tube. (a) In the case of $P = 1.2$ MPa and (b) in the case of $P = 0.8$ Mpa.

line, a dashed line, a chain line, a double dotted chain line, a thin solid line and a thick solid line also represent the correlations of the homogeneous model, Smith (1971), Zivi (1964), Baroczy (1966), Yashar et al. (2001), ($G = 180\ \mathrm{kg\,m^{-2}\,s^{-1}}$) and Yashar et al. (2001) ($G = 90\ \mathrm{kg\,m^{-2}\,s^{-1}}$), respectively. All of correlations for smooth tube show higher values than the present experimental data of microfin tube. This fact suggests that any correlations for smooth tube are not suitable to predict the void fraction in microfin tube. That is, the effect of grooves should be considered. The correlation of Yashar et al. (2001) for microfin tube also over-predicts the present data. They reported that there is no difference in void fraction between Smooth and microfin tubes. However, it is well known that the frictional pressure drop in a microfin tube is higher than that of a smooth tube. This suggests that mean liquid velocity in a microfin tube is lower than that of a smooth

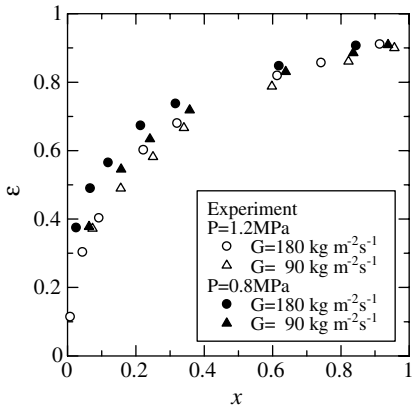

Fig. 5. Experimental results of void fraction for a microfin tube.

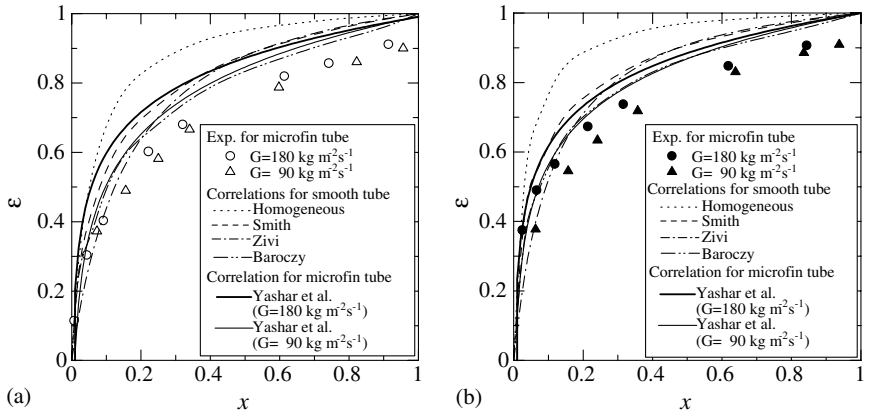

Fig. 6. Comparison between present experimental results and previous correlations for a microfin tube. (a) In the case of $P = 1.2$ MPa and (b) in the case of $P = 0.8$ MPa.

tube. Therefore, the void fraction in a microfin tube is supposed to be lower than that of a smooth tube.

Fig. 7(a) and (b) show the comparison between the experimental data for smooth and microfin tubes in the cases of $P = 1.2$ and 0.8 MPa, respectively. The influence of mass velocity on void fraction is observed apparently for microfin tube, compared with for smooth tube. There is also a distinction that the void fraction of a microfin tube becomes much lower than that of a smooth tube at the same vapor quality, especially in the high vapor quality region. This may be explained as follows:

The mean wall shear stress in a microfin tube becomes larger than that in a smooth tube because of the enlargement of wall area in microfin tube. Therefore, the bulk velocity of liquid decreases and the cross-sectional area occupied by liquid increases.

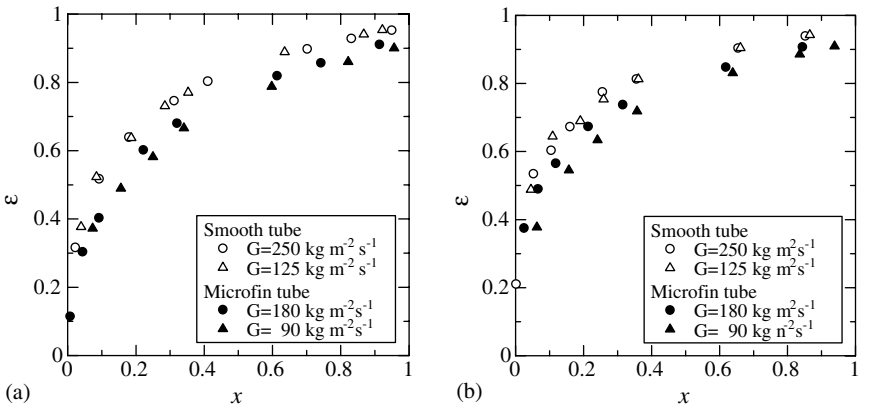

Fig. 7. Comparison of void fraction between a smooth and a microfin tubes. (a) In the case of $P = 1.2$ MPa and (b) in the case of $P = 0.8$ MPa.

4. A prediction method of void fraction for microfin tube

The prediction results by previous correlations for smooth tube are higher than the present experimental data of a microfin tube at adiabatic condition (see Fig. 6(a) and (b)). Therefore, a new prediction method for void fraction in a microfin tube is developed by combining a stratified-annular and annular flow models that are constructed from an observation of flow patterns and consideration of geometrical configuration of microfin tube. The effect of entrainment and gravitational force are neglected in the present method.

4.1. Stratified-annular flow model

Fig. 8 shows the schematic view of the stratified-annular flow model. The stratified-annular flow model is assumed that most of liquid flows at the bottom of tube and upper part of grooves is filled fully with additional liquid. Region of the bottom of the tube, where the most of liquid flows, is named liquid region II, while region of upper part of grooves, where additional liquid flows, is named liquid region I. In Fig. 8, n_1 is number of fins corresponding to liquid region I, A_{L1} is the total area of liquid region I, A_{L2} is the total area of liquid region II, A_G is the total area of vapor region, S_{L1} is the total perimeter of liquid region I, S_{L2} is the total perimeter of liquid region II, S_{i1} is the total perimeter between liquid region I and vapor region, S_{i2} is the total perimeter between liquid region II and vapor region and S_G is the total perimeter between vapor region and grooves. It is noted that the void fraction is smaller than the value of A_i/A in this model, where A_i is the area based minimum diameter of microfin tube and A is the area based mean inside diameter of microfin tube.

4.1.1. Liquid region I

Momentum equation of liquid in upper part of grooves is expressed as

$$PA_{L1} - (P + dP)A_{L1} - \tau_{L1}S_{L1}\,dz + \tau_{i1}S_{i1}\,dz = 0, \tag{5}$$

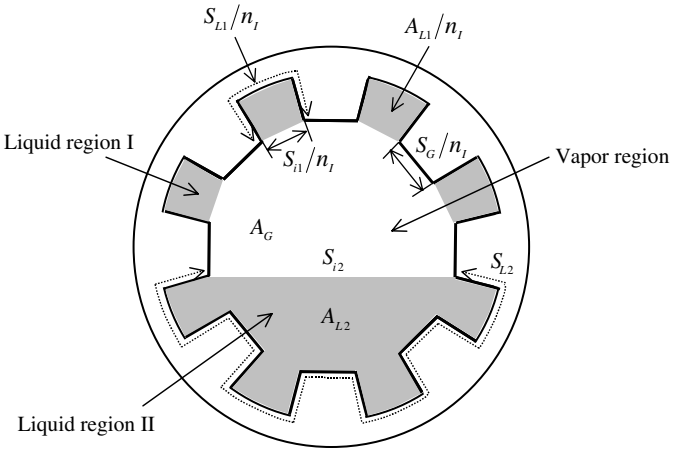

Fig. 8. Schematic view of the stratified-annular flow model.

where P is the pressure, dP is the infinitesimal pressure difference, dz is the infinitesimal length in the axial direction, τ_{L1} is the shear stress for liquid region I to tube wall and τ_{i1} is the shear stress between liquid region I and vapor region.

4.1.2. Liquid region II

Momentum equation of liquid at the bottom part of tube is expressed as

$$PA_{L2} - (P + dP)A_{L2} - \tau_{L2}S_{L2}\,dz + \tau_{i2}S_{i2}\,dz = 0, \tag{6}$$

where τ_{L2} is the shear stress for liquid region II to tube wall and τ_{i2} is the shear stress between liquid region II and vapor region.

4.1.3. Vapor region

Momentum equation of vapor core is expressed as

$$PA_G - (P + dP)A_G - \tau_{i1}S_{i1}\,dz - \tau_{i2}S_{i2}\,dz - \tau_G S_G\,dz = 0. \tag{7}$$

Rearranging Eqs. (5)–(7), the following equations are obtained:

$$-\frac{dP}{dz} = \frac{1}{A_{L1}}(\tau_{L1}S_{L1} - \tau_{i1}S_{i1}), \tag{5'}$$

$$-\frac{dP}{dz} = \frac{1}{A_{L2}}(\tau_{L2}S_{L2} - \tau_{i2}S_{i2}), \tag{6'}$$

$$-\frac{dP}{dz} = \frac{1}{A_G}(\tau_{i1}S_{i1} + \tau_{i2}S_{i2} + \tau_G S_G). \tag{7'}$$

Eliminating the pressure drop term from Eqs. (5′) and (7′), Eq. (8) can be obtained as

$$f_{L1}\rho_L u_{L1}^2 \frac{S_{L1}}{A_{L1}} - \rho_G u_G^2 \left(f_{i1}\frac{S_{i1}}{A_{L1}} + f_{i1}\frac{S_{i1}}{A_G} + f_{i2}\frac{S_{i2}}{A_G} + f_G\frac{S_G}{A_G} \right) = 0, \tag{8}$$

where f_{L1} is the friction factor in liquid region I, f_{i1} is the friction factor of interface between liquid region I and vapor region, f_{i2} is the friction factor of interface between liquid region II and vapor region, f_G is the friction factor in vapor region, u_G is the vapor velocity in vapor region and u_{L1} is the liquid velocity in liquid region I. The following equation is also obtained from equations Eqs. (6′) and (7′).

$$f_{L2}\rho_L u_{L2}^2 \frac{S_{L2}}{A_{L2}} - \rho_G u_G^2 \left(f_{i2} \frac{S_{i2}}{A_{L2}} + f_{i1} \frac{S_{i1}}{A_G} + f_{i2} \frac{S_{i2}}{A_G} + f_G \frac{S_G}{A_G} \right) = 0, \tag{9}$$

where f_{L2} is the friction factor in liquid region II and u_{L2} is the liquid velocity in liquid region II. The definition of friction factors, shear stresses and hydraulic diameters in these equations is summarized in Table 5. In Table 5, A_n is the area based on maximum diameter of microfin tube, γ is the helix angle of grooves for microfin tube, d_{L1} is the hydraulic diameter in liquid region I, d_{L2} is the hydraulic diameter in liquid region II, d_G is the hydraulic diameter in vapor region, Re_{L1} is the liquid Reynolds number in liquid region I, d_m is the mean inside diameter of a microfin tube and P_{groove} is the axial pitch of a groove in a microfin tube. In stratified-annular flow model, it is assumed that f_{i1}, f_{i2} and f_G are estimated by the Colburn correlation and f_{L2} is estimated by the Carnavos correlation (1980). f_{L1} is estimated by the correlation obtained by the preliminary experiment in which the pressure drop in a spiral smooth circular tube from 0.5 to 1.0 mm in inside diameter was measured.

The equation for conservation of mass in the tube can be written as

$$W = A_{L1}\rho_L u_{L1} + A_{L2}\rho_L u_{L2} + A_G \rho_G u_G. \tag{10}$$

To solve the coupled equations (8)–(10) for stratified-annular flow model, numerical calculation was carried out based on the following step by step procedures

(1) Geometrical configurations of microfin tube, physical properties of R134a and mass flow rate are given as known values.
(2) The value of void fraction is given as a known value. Total area occupied by liquid $A_L (= A_{L1} + A_{L2})$, total area occupied by vapor A_G, perimeters and hydraulic diameters can be calculated.
(3) Assuming the initial vapor velocity u_G in given void fraction, u_{L1} and u_{L2} can be calculated from Eqs. (8) and (9), respectively.
(4) If the convergence condition between calculated mass flow rate in Eq. (10) and given mass flow rate is satisfied, vapor quality can be calculated in given void fraction.
(5) If calculated velocities do not satisfy the convergence condition, assuming the new vapor velocity u_G and iterate the procedure from (3) to (4) until the convergence condition is satisfied.

4.2. Annular flow model

Fig. 9 shows the schematic view of annular flow model. In annular flow model, all grooves are assumed to be filled with liquid uniformly with refrigerant flow height H_R. In Fig. 9, n is the number of fins of microfin tube, A_L is the total area of liquid region, A_G is the total area of vapor region, S_L is the total perimeter of liquid region, S_i is the total perimeter between liquid region and

Table 5
Definition of shear stresses, friction factors and hydraulic diameters employed in the present prediction method

Stratified-annular flow model	Annular flow model
Shear stresses	
$\tau_{L1} = f_{L1}(\rho_L u_{L1}^2)/2$	$\tau_L = f_L(\rho_L u_L^2)/2$
$\tau_{L2} = f_{L2}(\rho_L u_{L2}^2)/2$	$\tau_i = f_i(\rho_G u_G^2)/2$
$\tau_{i1} = f_{i1}(\rho_G u_G^2)/2$	$\tau_G = f_G(\rho_G u_G^2)/2$
$\tau_{i2} = f_{i2}(\rho_G u_G^2)/2$	
$\tau_G = f_G(\rho_G u_G^2)/2$	
Friction factors	
$f_{L1} = \left(1 + \left(\frac{6.89\times10^{-3}}{(P_{groove}/d_m)^{0.74}}\right)\cdot\left(Re_{L1}\cdot\left(\frac{d_{L1}}{d_m}\right)^{1/2}\right)^{1.18}\right)^{\frac{1}{2}} \times \left(\frac{16}{Re_{L1}}\right)$	$f_L = \left(1 + \left(\frac{6.89\times10^{-3}}{(P_{groove}/d_m)^{0.74}}\right)\cdot\left(Re_L\cdot\left(\frac{d_L}{d_m}\right)^{1/2}\right)^{1.18}\right)^{\frac{1}{2}} \times \left(\frac{16}{Re_L}\right)$
where $P_{groove} = (2\pi(d_m/2))/\tan\gamma$	where $P_{groove} = (2\pi(d_m/2))/\tan\gamma$
$f_{L2} = 0.046(\rho_L d_{L2} u_{L2}/\eta_L)^{-0.2}(A/A_n)^{0.5}(\sec\gamma)^{0.75^*}$	$f_i = 0.046(\rho_G d_G u_G/\eta_G)^{-0.2}$
$f_{i1} = 0.046(\rho_G d_G u_G/\eta_G)^{-0.2}$	$f_G = 0.046(\rho_G d_G u_G/\eta_G)^{-0.2}(A/A_n)^{0.5}(\sec\gamma)^{0.75^*}$
$f_{i2} = 0.046(\rho_G d_G u_G/\eta_G)^{-0.2}$	
$f_G = 0.046(\rho_G d_G u_G/\eta_G)^{-0.2}$	
Hydraulic diameters	
$d_{L1} = \frac{4A_{L1}}{S_{L1}}, \quad d_{L2} = \frac{4A_{L2}}{S_{L2}}, \quad d_G = \frac{4A_G}{S_G + S_i}$	$d_G = \frac{4A_G}{S_G + S_i}, \quad d_L = \frac{4A_L}{S_L}$

*Proposed by Carnavos (1980) for microfin tube.

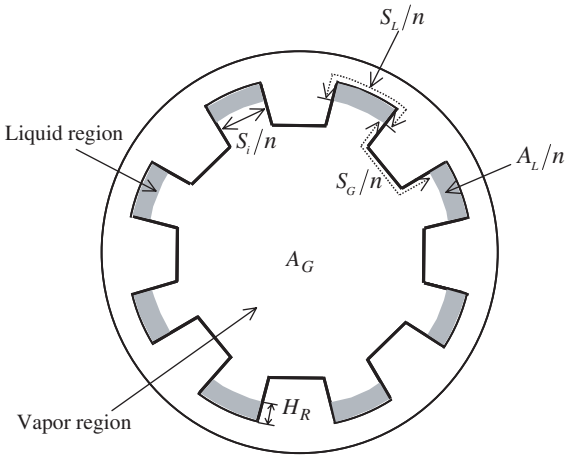

Fig. 9. Schematic view of the annular flow model.

vapor region, S_G is the total perimeter between grooves and vapor region and H_R is the height of refrigerant flow inside grooves. It is noted that the void fraction is larger than the value of A_i/A in this model.

4.2.1. Liquid region

Momentum equation of liquid in grooves is expressed as

$$PA_L - (P + dP)A_L - \tau_L S_L dz + \tau_i S_i dz = 0, \tag{11}$$

where τ_L is the shear stress between liquid region and tube wall and τ_i is the shear stress between liquid region and vapor region.

4.2.2. Vapor region

Momentum equation of vapor core is expressed as

$$PA_G - (P + dP)A_G - \tau_G S_G dz - \tau_i S_i dz = 0, \tag{12}$$

where τ_G is the shear stress in vapor region.

Rearranging Eqs. (11) and (12), the following equations are obtained:

$$-\frac{dP}{dz} = \frac{1}{A_L}(\tau_L S_L - \tau_i S_i), \tag{11'}$$

$$-\frac{dP}{dz} = \frac{1}{A_G}(\tau_G S_G + \tau_i S_i). \tag{12'}$$

Eliminating the pressure drop term from Eqs. (11′) and (12′), Eq. (13) can be obtained

$$f_G \rho_G u_G^2 \frac{S_G}{A_G} - f_L \rho_L u_L^2 \frac{S_L}{A_L} + f_i \rho_G u_G^2 S_i \left(\frac{1}{A_G} + \frac{1}{A_L}\right) = 0, \tag{13}$$

where f_L is the friction factor in liquid region, f_G is the friction factor in vapor region, u_L is the liquid velocity in liquid region and u_G is the vapor velocity in vapor region. The definition of

friction factors and shear stresses in these equations are summarized in Table 5, where d_L is the hydraulic diameter in liquid region, d_G is the hydraulic diameter in vapor region and Re_L is the liquid Reynolds number in liquid region. In annular flow model, it is assumed that f_i is estimated by the Colburn correlation and f_G are estimated by the Carnavos correlation. f_L is estimated by the correlation in preliminary experiment that was proposed for the pressure drop in a spiral smooth circular tube from 0.5 to 1.0 mm in inside diameter.

The equation for conservation of mass in the tube is expressed as

$$W = A_L \rho_L u_L + A_G \rho_G u_G. \tag{14}$$

The coupled Eqs. (13) and (14) are solved using the similar method as for stratified-annular flow model.

4.3. Comparison between experimental data and calculation results

Fig. 10(a) and (b) show the comparison between the experimental data for microfin tube and prediction result by the present prediction method in the cases of $P = 1.2$ and 0.8 MPa, respectively. The values of the predicted the void fraction are in good agreement with experimental data in high vapor quality region, while the predicted values are slightly smaller than experimental ones in low vapor quality region.

Fig. 11(a)–(d) show the comparison between experimental and predicted mean velocities. Symbols of opened and closed circles denote experimental mean liquid velocity, $u_{L,mean}$, and experimental mean vapor velocity, $u_{G,mean}$, respectively. A chain line and a double dotted chain line denote the predicted mean liquid and vapor velocities, respectively. As reference, in each figure, the predicted liquid velocity in Region I, u_{L1}, and the predicted liquid velocity in Region II, u_{L2}, of stratified-annular flow model are also plotted by a solid and a dashed lines, respectively. The values of predicted mean liquid velocity $u_{L,mean}$, are in good agreement with experimental ones. However, the values of predicted mean vapor velocity, $u_{G,mean}$, is slightly higher value than

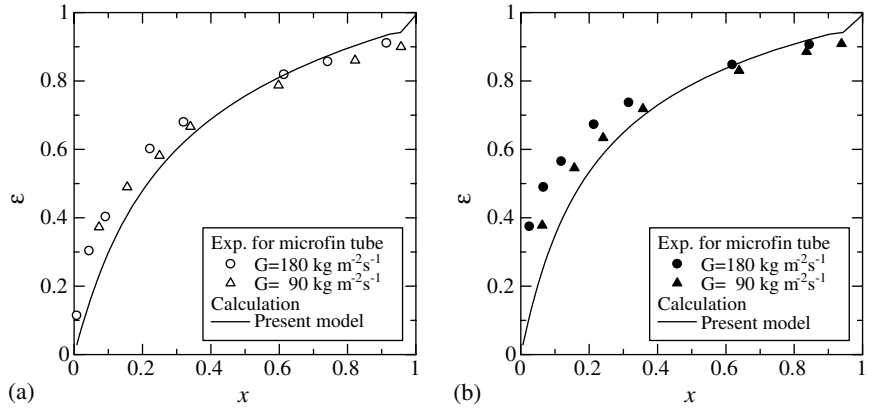

Fig. 10. Comparison between experimental and calculation results of void fraction for a microfin tube. (a) In the case of $P = 1.2$ MPa and (b) in the case of $P = 0.8$ MPa.

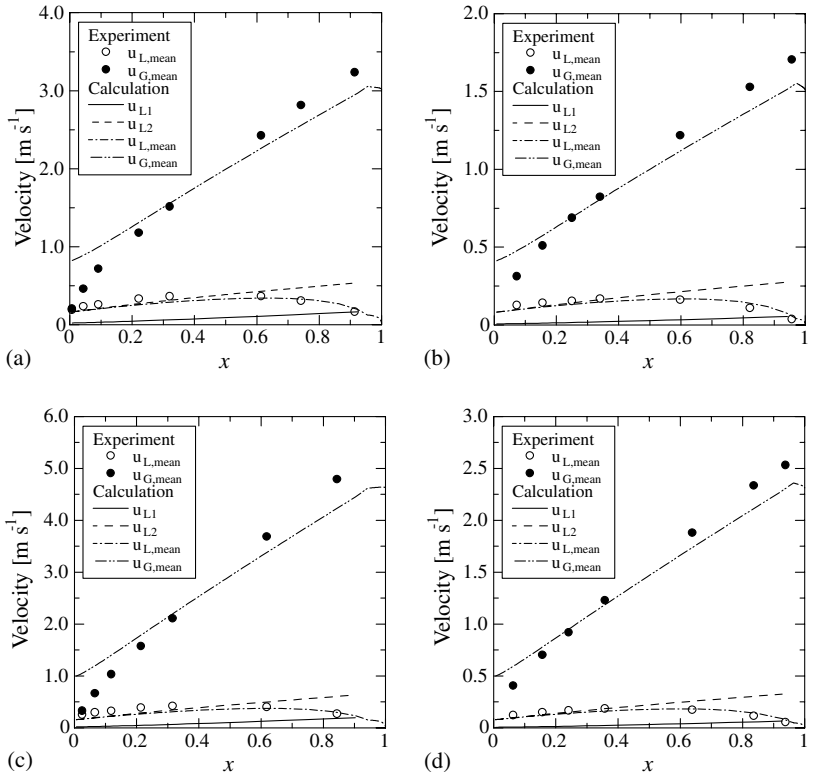

Fig. 11. Comparison between experimental and predicted mean velocities for varying pressure and mass velocity. (a) $P = 1.2$ MPa, 180 kg m^{-2} s^{-1}, (b) $P = 1.2$ MPa, 90 kg m^{-2} s^{-1}, (c) $P = 0.8$ MPa, 180 kg m^{-2} s^{-1} and (d) $P = 0.8$ MPa, 90 kg m^{-2} s^{-1}.

the experimental ones in low vapor quality region and slightly lower than the experimental ones in high vapor quality region. It appears that this discrepancy between predicted mean vapor velocity and experimental one is mainly due to difference between real flow pattern and present flow model. However, the present prediction method would be of a great interest to investigate the two-phase flow phenomena in a microfin tube. This method will also be useful to design heat exchangers in air-conditioning and refrigerating systems.

5. Conclusions

The experiments on the void fraction of refrigerant R134a two-phase flow in smooth and microfin tubes were carried out at adiabatic condition. A new approach to predict void fraction was conducted for microfin tube. The main results obtained are as follows:

(1) The void fraction for both smooth and microfin tubes increases with the decrease in refrigerant pressure.

(2) The effect of the mass velocity on the void fraction in microfin tube is more remarkable than that of smooth tube.
(3) The void fraction for a microfin tube is lower than that for a smooth tube at the same experimental condition including pressure, mass velocity and vapor quality. This fact suggests that any correlations for a smooth tube are not suitable to predict the void fraction in a microfin tube.
(4) The mean shear stress of liquid to tube wall in a microfin tube becomes larger than that in a smooth tube. Therefore, the bulk velocity of liquid decreases and the cross-sectional area occupied by liquid increases.
(5) The void fraction for a smooth tube can be predicted well by the Smith or the Baroczy correlations.
(6) A prediction method for void fraction in a microfin tube is constructed from momentum equations of stratified-annular and annular flow models. The values of the predicted the void fraction are in good agreement with experimental data in high vapor quality region, while the predicted values are slightly smaller than experimental ones in low vapor quality region.
(7) The present prediction method gives good information of two-phase flow phenomena in a microfin tube and could be available for practical applications.

References

Baroczy, C.J., 1966. A systematic correlation for two-phase pressure drop. Chemical Engineering Progress Symposium series 62, 232–249.

Butterworth, D., 1975. A comparison of some void fraction relationships for co-current gas–liquid flow. Int. J. Multiphase Flow 1, 845–850.

Carnavos, T.C., 1980. Heat transfer performance of internally finned tubes in turbulent flow. Heat Transfer Engineering 1, 32–37.

Hughmark, G.A., 1962. Holdup in gas–liquid flow. Chemical Engineering Progress 58, 62–65.

Levy, S., 1960. Steam slip-theoretical prediction from momentum model. J. Heat Transfer, 113–124.

Lockhart, R.W., Martinelli, R.C., 1949. Proposed correlation of data for isothermal two-phase, two-component flow in pipes. Chemical Engineering Progress 45, 39–49.

Moffat, R.J., 1988. Describing the uncertainties in experimental results. Experimental Thermal and Fluid Science 1, 3–17.

NIST, 1998. NIST Thermodynamic and transport properties of refrigerants and refrigerant mixtures-REFPROP Version 6.0. National Institute of Standards and Technology.

Premoli, A., Francesco, D.D., Prina, A., 1971. A dimensional correlation for evaluating two-phase mixture density. La Termotecnica 25, 17–26.

Rice, C.K., 1987. The effect of void fraction correlation and heat flux assumption on refrigerant charge inventory predictions. ASHRAE Transactions 93 (Part I), 341–367.

Smith, S.L., 1971. Void fractions in two-phase flow: a correlation based upon an equal velocity head model. Heat and Fluid Flow 1, 22–39.

Tandon, T.N., Varma, H.K., Gupta, C.P., 1985. A void fraction model for annular two-phase flow. Int. J. Heat and Mass Transfer 28, 191–198.

Thom, J.R.S., 1964. Prediction of pressure drop during forced circulation boiling of water. Int. J. Heat and Mass Transfer 7, 709–724.

Wallis, G.B., 1969. One-dimensional two-phase flow. McGraw-Hill, New York. pp. 51–54.

Yashar, D.A., Wilson, M.J., Kopke, H.R., Graham, D.M., Chato, J.C., Newell, T.A., 2001. An investigation of refrigerant void fraction in horizontal, micro-fin tubes. International Journal of HVAC & R Research 107 (Part 2), 173–188.

Zivi, S.M., 1964. Estimation of steady-state steam void fraction by means of the principle of minimum entropy production. J. Heat Transfer 86, 247–252.